Proximity Mapping of the Tet Repressor−Tetracycline−Fe^{2+} Complex by Hydrogen Peroxide Mediated Protein Cleavage†

Norbert Ettner,‡ Jörg W. Metzger,§ Thomas Lederer,‡ Jeffrey D. Hulmes,|| Caroline Kisker,⊥ Winfried Hinrichs,⊥ George A. Ellestad,⊥ and Wolfgang Hillen*,‡

Lehrstuhl für Mikrobiologie, Institut für Mikrobiologie und Biochemie der Friedrich-Alexander Universität Erlangen-Nürnberg, Staudtstrasse 5, 91058 Erlangen, FRG, Institut für Organische Chemie, Universität Tübingen, Auf der Morgenstelle 18, 72076 Tübingen, FRG, Lederle Laboratories, Medical Research Division, American Cyanamid Company, Pearl River, New York 10965, and Institut für Kristallographie, Freie Universität Berlin, Takustrasse 6, 14195 Berlin, FRG

Received May 4, 1994; Revised Manuscript Received September 21, 1994®

ABSTRACT: We demonstrate in a quantitative *in vitro* induction assay that tetracycline−Fe^{2+} is a more than 1000-fold stronger inducer of Tet repressor compared to tetracycline−Mg^{2+}. Oxidative cleavage of the Tet repressor−tetracycline−Fe^{2+} complex with H_2O_2 and ascorbate results in an Fe^{2+}-dependent specific fragmentation of the protein. The maximal yield of about 15% and a reaction time of less than 30 s are only observed in the presence of the drug, whereas about 1% cleavage is obtained after 30 min in the presence of Fe^{2+} without tetracycline. Cleavage is not inhibited by several radical scavengers, suggesting a highly localized reactivity of the redox-active oxo intermediates in the proximity of the Fe^{2+}−tc chelater where they are generated. The products can be separated by HPLC only after denaturation, indicating that the complex is not disrupted by cleavage. Residues at which the cleavage takes place are identified using the masses of the fragments determined by electrospray mass spectrometry and their N-terminal sequences. The major cleavage site maps to residues 104 and 105 of Tet repressor. Less efficient cleavages occur at residues 56 and 136, and the least efficiently cleaved sites are around residues 144 and 147. The cleavage efficiencies correlate to the distances and orientations of the respective peptide bonds to Mg^{2+} in the crystal structure of the Tet repressor−tetracycline−Mg^{2+} complex. We discuss potential reaction mechanisms leading to protein cleavage.

A prominent mechanism of resistance to tetracycline (tc) antibiotics in Gram-negative bacteria is mediated by a membrane-residing protein which couples the export of a tc−M^{2+} complex to the import of a proton (Yamaguchi et al., 1990). Expression of the tc efflux protein from Tn10 is controlled by a dimeric Tet repressor protein consisting of 207 amino acids per monomer (Postle et al., 1984) which links transcription to the presence of the drug (Beck et al., 1982) by tc-sensitive, sequence-specific binding to *tet* operator DNA (Bertrand et al., 1983; Hillen et al., 1982, 1983, 1984). tc has a high affinity for Tet repressor (K_{assoc} = 3 × 10^9 M^{-1}; Takahashi et al., 1991), meeting the requirement that induction of resistance must be very efficient to assure expression of the efflux protein prior to inhibition of protein synthesis. Noninducible mutations of the Tet repressor have been obtained at a large number of residues spanning the major portion of the primary structure (Smith & Bertrand, 1988; Hecht et al., 1993). This result indicates that many residues of TetR contribute to tc binding and/or induction. It is the goal of this study to obtain biochemical evidence to further define the tc binding pocket of TetR.

Binding of tc to the repressor and induction of expression of the efflux protein depend strictly on the presence of divalent cations like Mg^{2+}, which can be replaced by a number of other divalent ions (Takahashi et al., 1986). Six Tet repressor sequence variants have been characterized so far, encoded in different tc resistance determinants isolated from various bacteria (Hillen & Berens, 1994). Two of these are compared in this study, which has been performed using the Tn10-encoded Tet repressor called TetR(B). X-ray studies were recently successful using the R-factor RA1-encoded Tet repressor called TetR(D) (Unger et al., 1984; Hinrichs et al., 1994). They share 65% identical residues and are, thus, regarded as isostructural and isofunctional proteins (Hinrichs et al., 1994). The crystal structure of the TetR(D)−tc−Mg^{2+} complex reveals an octahedral coordination of Mg^{2+}, which involves O(11) and O(12) from tc, the His100 imidazole side chain from TetR, and three water molecules, two of which are held in place by specific interactions with the protein (Hinrichs et al., 1994).

Fenton chemistry using Fe^{2+}-EDTA and H_2O_2 to generate highly reactive oxo intermediates in the vicinity of Fe^{2+} has been successfully applied during the past several years to map solvent-accessible residues in nucleic acids (Tullius & Dombroski, 1986; Dixon et al., 1991). In an attempt to extend this approach to the analysis of proteins, EDTA has been tethered either to an amino acid residue (Rana & Meares, 1990, 1991a,b; Ermácora et al., 1992) or to substrates (Schepartz & Cuenoud, 1990; Hoyer & Schultz., 1990) to direct Fe^{2+} to the vicinity of these sites and map proximal residues by analyzing the resulting cleavage

† This work was supported by grants from the Wilhelm Sander Stiftung and the Deutsche Forschungsgemeinschaft to J.W.M. through SFB 323.

* Author to whom correspondence should be addressed.
‡ Friedrich-Alexander Universität Erlangen-Nürnberg.
§ Universität Tübingen.
|| American Cyanamid Co.
⊥ Freie Universität Berlin.

® Abstract published in *Advance ACS Abstracts,* December 1, 1994.

0006-2960/95/0434-22$09.00/0

products. We have shown recently that Fe^{2+}-dependent oxidative cleavage of the TetR(B)−tc−Fe^{2+} complex leads to specific fragmentation of the repressor protein (Ettner et al., 1993).

We report here the *in vitro* induction of Tet repressor by tc−Fe^{2+} demonstrating that Fe^{2+} can be part of the biologically active inducer. Fe^{2+}-dependent oxidative cleavage of Tet repressor is, thus, the first time that this approach is performed using an unmodified substrate. Extensive analyses of the cleaved peptides by electrospray mass spectroscopy (ESMS) and N-terminal sequencing yield a detailed map of residues located proximal to Fe^{2+} in the induced form of TetR complexed with tc−Fe^{2+}.

MATERIALS AND METHODS

Materials. All reagents and solvents were of the highest purity available. Milli-Q water was used for all aqueous reactions and dilutions. Buffer A contained 0.5 M NaCl and 0.2 M Tris-HCl (pH 7.0); buffer B contained 2.5% (w/v) SDS, 32 mM DTT, 80 μM EDTA, 0.1% (w/v) bromophenol blue, and 0.4 M Tris-HCl (pH 8.0). Hydrogen peroxide was purchased from Sigma, St. Louis, MO, and sodium ascorbate and monoperoxyphthalic acid, magnesium salt, were from Aldrich, Steinheim, FRG. $(NH_4)_2Fe(SO_4)_2$ was a product of E. Merck, Darmstadt, FRG. Tc and tc analogs were provided by Lederle Laboratories, Pearl River, NY.

Isolation and Purification of Tet Repressor. *Escherichia coli* W3110 was transformed with pWH1950 containing *tetR* under *tac* promoter control. The protein was isolated from a 1.5-L culture of this strain induced with 1.5 mM IPTG and purified to homogeneity as described in detail elsewhere.

Fluorescence Measurements. The binding activity of tc to Tet repressor was determined by tc and protein fluorescence using a Spex fluorometer (Spex Industries, Edison, NJ) equipped with two double monochromators by measuring the fluorescence of the drug at 520 nm after excitation at 376 nm (Takahashi et al., 1986).

Cleavage of Tet Repressor with H_2O_2. The cleavage reaction was performed in a total volume of 30 μL of buffer A. The concentration of Tet repressor monomer was 22 μM. A Tet repressor solution was incubated with an equimolar amount of $(NH_4)_2Fe(SO_4)_2$ and a 2-fold excess of tc for 3 min at room temperature. A 10-fold excess of sodium ascorbate was then added, immediately followed by a 10-fold excess of H_2O_2, each over Fe^{2+}. This mixture was incubated for 15 s at ambient temperatures, and then 3 μL of a 60% (w/v) solution of glycerol in water and 20 μL of buffer B were added to stop the reaction. The mixture was heated for 5 min in boiling water. Then 3 μL of a 20% (w/v) 2-iodoacetamide solution was added, and the mixture was incubated for 5 min at ambient temperatures. H_2O_2 titrations were performed under identical conditions except that H_2O_2 was added to a final concentration of 11, 22, 33, 55, 110, and 220 μM, respectively. Ascorbate titrations were carried out in the presence of 0.22 mM H_2O_2 in buffer A, and ascorbate was added to final concentrations of 11, 22, 33, 55, 110, and 220 μM. Cleavage reactions also were carried out in the presence of the radical scavengers glycerol, *tert*-butyl alcohol, mannitol, and thiourea at final concentrations of 0.5 M in buffer A. The reagents were added to the mixture of Tet repressor and tc−Fe^{2+} and incubated for 3 min before addition of ascorbate and H_2O_2.

In Vitro Induction Assay. A 204-bp DNA fragment containing *tet* operator O_1 was prepared from pWH964 (Niederweis et al., 1992) as described (Tovar & Hillen, 1991). The fragment was end-labeled on one side using [γ-^{32}P]ATP as described (Maxam & Gilbert, 1980). One picomole of fragment containing 20 000 cpm was incubated in 40 μL of 20 mM Tris-HCl, pH 8.0, 4.3 pmol of Tet repressor, 1.1 nmol of tc, 10 μg of nonspecific DNA, and different amounts of $MgCl_2$ or $(NH_4)_2Fe_2(SO_4)_2$ at ambient temperatures for 30 min. Methylation, cleavage of methylated DNA, and gel electrophoresis of the products was accomplished as described (Heuer & Hillen, 1988). Autoradiography was done using Hyperfilm-MP (Amersham, Braunschweig, FRG) for 24 h with an intensifying screeen. The autoradiographs were densitometrically scanned using Ultrascan XL (Pharmacia LKB, Freiburg, FRG). The intensity of the G(2) band in *tet* operator was then normalized using the intensities of bands of two G residues which are not affected by Tet repressor binding. The induction was defined to be 0% in the absence of tc and 100% in the absence of Tet repressor.

Time Course and Quantification of Fe^{2+}-Mediated Cleavage in the Presence and Absence of tc. The time courses of Tet repressor cleavage with Fe^{2+} or tc−Fe^{2+} were determined by the addition of 18 μM Fe^{2+} and 36 μM tc, respectively, to 18 μM Tet repressor. Both reaction mixtures were incubated for 3 min at ambient temperatures with continuous stirring. Then 0.27 mM sodium ascorbate and 5.4 mM H_2O_2 were added to give a final volume of 3.0 mL. Aliquots of 450 μL (170 μg of protein) were taken from each sample at 0.25, 0.5, 1, 2, 5, 10, and 30 min and added to 400 μL of a solution containing 5 M urea, 32 μM DTT, and 0.5 M glycerol. After denaturation of the proteins in boiling water for 5 min, 30 μL of a 20% (w/v) 2-iodoacetamide solution was added, and the samples were applied to a C_4 reverse-phase HPLC column.

SDS−PAGE and Amino-Terminal Sequence Analysis. Protein SDS−PAGE (Schägger & von Jagow, 1987) was run on a Pharmacia, Freiburg, FRG, PhastSystem using precast PhastGel high-density gels [20% acrylamide, 2% bis-(acrylamide), and 30% ethylene glycol]. Gels were run for approximately 35 min (215 V h) and stained with either silver (Heukeshoven & Dernick, 1988) or Coomassie blue in the development unit of the PhastSystem. Cleaved fragments were blotted onto ProBlot PVDF membrane (Applied Biosystems) by a Pharmacia PhastTransfer unit and stained with Coomassie blue. N-Terminal sequences were determined by automated Edman degradation, using an Applied Biosystems, Foster City, CA, 477A pulsed liquid sequencer.

HPLC Purification of Protein Fragments. Tet repressor (17.9 μM) was incubated either with equimolar amounts of Fe^{2+} as a control or together with a 2-fold excess of tc in a total volume of 3 mL of buffer A for 3 min and treated with 0.27 mM sodium ascorbate and 1.8 mM H_2O_2 for 1 min. The cleavage reaction was stopped by addition of deionized urea to a concentration of 5 M and DTT to 35 mM, before the samples were denatured in boiling water for 5 min. The reaction mixtures were separated by reverse-phase chromatography using a Nucleosil 4 × 125 mm column (C_4, 5 μm, 300 Å) obtained from Macherey & Nagel, Düren, FRG, and a Pharmacia LKB HPLC pump and controller connected with a Knauer, Berlin, FRG, variable-wavelength monitor. Fractions containing cleaved fragments were rechromatographed

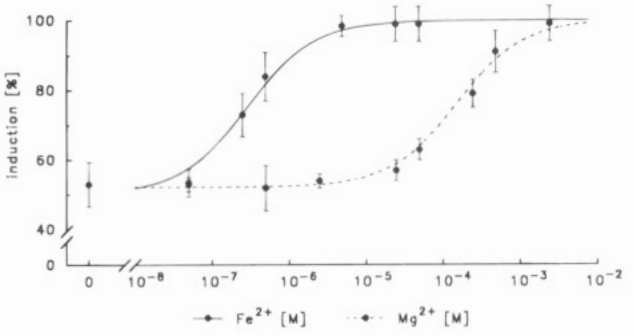

FIGURE 1: *In vitro* induction of TetR by tc−Mg^{2+} and tc−Fe^{2+}. The *in vitro* induction of TetR is shown as increasing methylation of G(2) in *tet* operator (see Materials and Methods) at different concentrations of Mg^{2+} (dashed line) and Fe^{2+} (solid line). The lines represent sigmoidal fits of the experimental data. Standard deviations indicated for each point were derived from repeat experiments. In the left part of the plot the induction without any addition of divalent metal ions is given. The concentration of TetR was 1×10^{-7} M (dimer) and of tc 5×10^{-5} M in all titration experiments.

on a Nucleosil 4 × 250 mm column (C_{18}, 5 μm, 120 Å). Prepared samples were acidified with trifluoroacetic acid (1%) and applied on a column equilibrated in solvent A (20% acetonitrile in 0.115% trifluoroacetic acid) at room temperature. After the samples were washed for 15 min elution was carried out with a linear gradient between solvents A and B (0−100% trifluoroacetic acid in 66% acetonitrile) over a 30-min period at a flow rate of 0.75 mL/min. The eluate was monitored at 215 nm.

Electrospray Mass Spectrometry. Positive ion mass spectra were recorded using a Sciex API III triple−quadrupole mass spectrometer (Sciex, Toronto, Canada). The mass spectrometer was equipped with a pneumatically assisted electrospray interface ("ion spray"; Bruins et al., 1987). For rapid analysis of numerous prepurified fractions a steep HPLC gradient (0−100% solvent B in 10 min) at a flow rate of 40 μL/min (on-line HPLC) was used to further purify the samples prior to mass spectrometry.

Model Building of the Cleavage Sites in TetR(D). Model building was accomplished on an Iris INDIGO (Silicon Graphics GmbH, Grasbrunn-Neukeferloh, FRG) graphic system with the programs Insight II (Biosym Technologies, San Diego, CA) and Showcase (Silicon Graphics) using the X-ray coordinates of TetR(D) (Hinrichs et al., 1994).

RESULTS

In Vitro Induction with tc−Fe^{2+}. We have devised an *in vitro* induction assay making use of Tet repressor binding dependent protection from methylation of G residues in *tet* operator (Heuer & Hillen, 1988). As the inducer tc is titrated to the repressor−operator complex, a gradual deprotection of *tet* operator is observed, which is densitometrically quantitated (details will be published elsewhere). In the absence of added divalent ions a basic induction corresponding to about 50% deprotection is observed upon addition of tc (see Figure 1), which can be reduced to 0% by adding EDTA (data not shown). Therefore, we attribute this elevated induction level to the presence of residual divalent cations in the Tet repressor preparation. Addition of excess Mg^{2+} or Fe^{2+} yields 100% induction in the presence of tc, indicating that divalent cations are the limiting factor in this experiment. No induction is seen after addition of excess

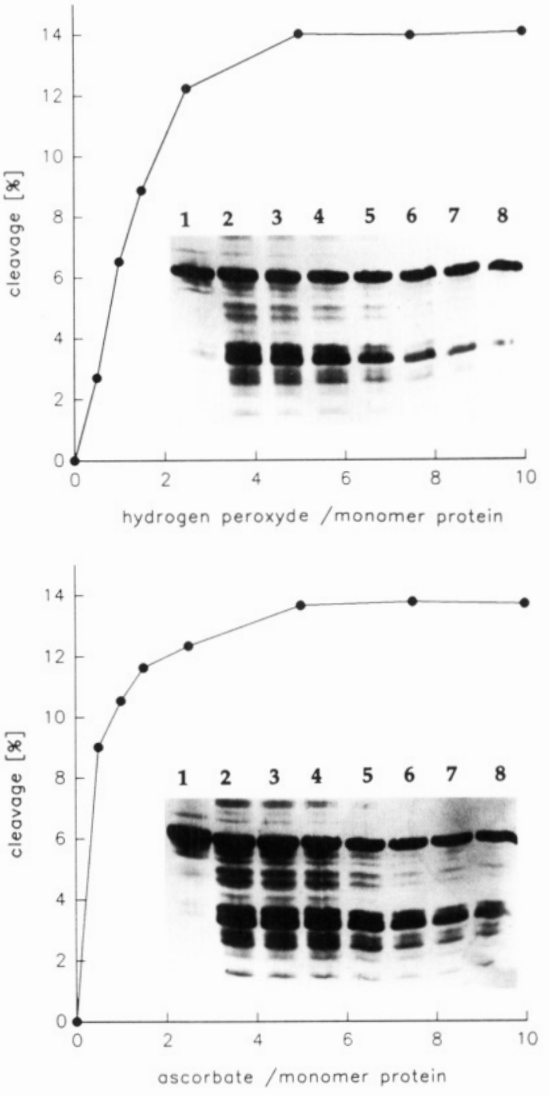

FIGURE 2: Efficiency of TetR cleavage depending on H_2O_2 and ascorbate. The yield of cleavage in percent of the total protein is plotted against the molar excess of H_2O_2 over Fe^{2+} and TetR monomer (A, top) and against the excess of ascorbate and TetR monomer (B, bottom), respectively. The insets show the respective silver-stained gels of each titration experiment. A 10-fold molar excess of ascorbate for (A) and H_2O_2 for (B) was added. Lane 1 of each gel: TetR and Fe^{2+} (11 μM) incubated with tc (22 μM) and without cleavage reagents. Lanes 2−8: as in lane 1 plus addition of a 10-, 7.5-, 5-, 2.5-, 1.5-, 1-, and 0.5-fold concentration of either H_2O_2 (A) or ascorbate (B), respectively.

amounts of Mg^{2+} or Fe^{2+} in the absence of tc (not shown). Fe^{2+} is about 1000-fold more efficient than Mg^{2+}, as half-induction with the former ion is seen at about 10^{-7} M, while about 10^{-4} M Mg^{2+} is needed to achieve half-induction in the titration experiment shown in Figure 1. Since the TetR concentration in this experiment is 2×10^{-7} M (given in dimers containing two binding sites), the 1000-fold increased efficiency of Fe^{2+}- over Mg^{2+}-mediated induction represents the lower limit of activity increase.

Efficient Protein Cleavage of TetR(B)−tc−Fe^{2+} Requires Ascorbate and H_2O_2. The protein cleavage reaction was investigated by either titrating with H_2O_2 in the presence of excess ascorbate (Figure 2A) or titrating with ascorbate in the presence of excess H_2O_2 (Figure 2B). The cleavage products were analyzed by SDS−PAGE. The respective densitometric analyses were performed by scanning the gels shown as inserts in Figure 2. Since the gels were silver-

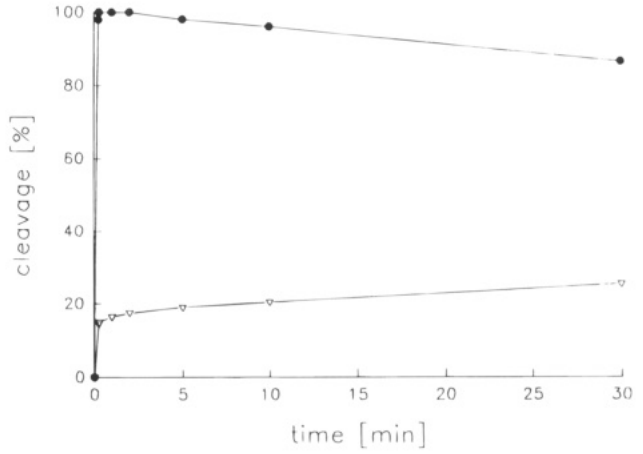

FIGURE 3: Time course of TetR cleavage. The different HPLC signal intensities of separated cleavage fragments in the presence of tc−Fe^{2+} (filled circles) and of Fe^{2+} (open triangles) are plotted versus the reaction time. The maximal cleavage efficiency is set to 100%.

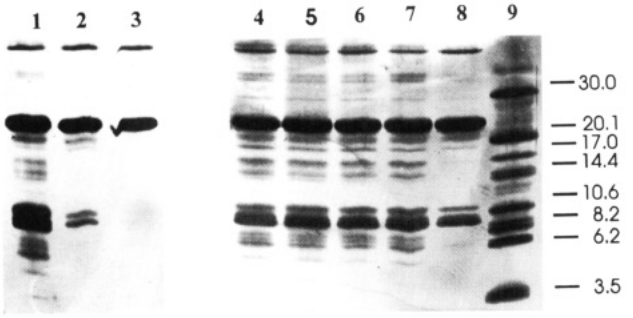

FIGURE 4: Gel analysis of the TetR cleavage products in the presence of tc−Fe^{2+} and Fe^{2+}. Silver-stained SDS−PAGE gels of the cleavage reactions are shown. Lanes: 1 and 4, TetR incubated with equimolar Fe^{2+} and a 2-fold excess of tc; 2, TetR incubated with an equimolar amount of Fe^{2+}; 3, TetR incubated with a 2-fold excess of tc without Fe^{2+}; 5−8, same as in lane 4 except that glycerol, *tert*-butyl alcohol, mannitol, and thiourea, respectively, were added at a concentration of 0.5 M each before addition of the cleavage reagents; 9, molecular weight marker. The concentration of TetR dimer was 11 μM in all the samples. Ascorbate/H_2O_2 was added to a concentration of 0.22 mM.

stained, this is more a visualization of the results than a reliable quantification. Nevertheless, these results indicate that both reagents are required for cleavage. Some cleavage occurred when either H_2O_2 or ascorbate was present in excess of the respective other component, but in submolar amounts relative to repressor and Fe^{2+}. Under these conditions only the most prominent cleavage bands at 10 and 9 kDa are observed. A 5-fold excess of H_2O_2 or ascorbate gave the highest yield of cleavage. Higher concentrations of both reagents did not result in further enhanced cleavage. It is noteworthy that an increase of specific cleavage is clearly detectable even in the presence of less than stoichiometric amounts of the reagents; however, to obtain the maximal yield, an excess of reagents is required. This indicates that the active oxo intermediate species has to be generated several times. Replacement of H_2O_2 by monoperoxyphthalic acid at 20 mM did not result in protein cleavage. Similarly, substitution of Fe^{2+} by Fe^{3+} in the absence of ascorbate did not result in appreciable cleavage of the protein (data not shown).

Cleavage of TetR−tc−Fe^{2+} Is a Fast Reaction. Time courses of TetR cleavage in the presence of tc−Fe^{2+} and Fe^{2+} are shown in Figure 3. Both reagents undergo a fast and a slow reaction with Tet repressor. Only about 15% of the cleavage products obtained with tc−Fe^{2+} are produced

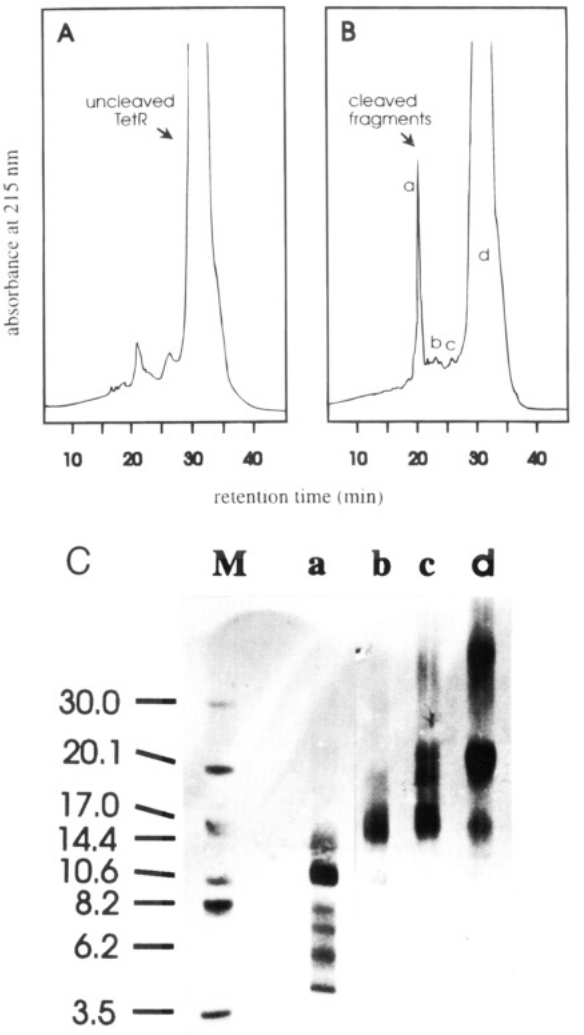

FIGURE 5: RP-HPLC purification of small cleaved fragments. TetR (17.9 μM) was treated with Fe^{2+} in the absence (A) or presence (B) of tc. The elution profiles were monitored at 215 nm. The material occurring in peaks a−d was analyzed by SDS−PAGE and silver-stained (C). Lanes: 1, molecular weight marker; 2, peak a; 3, peak b; 4, peak c; 5, peak d (diluted 1:10).

Table 1: ESMS Analysis of the Cleavage Products

determined masses[a]	assignment[b]	theoretical mass[c]
6 136 ± 2.4	Ser2−Ala56	6 143
6 139 ± 3.3		
11 705 ± 3.5	Ser2−Arg104	11 757
11 699 ± 3.1		
11 745 ± 5.8		
11 436[d] ± 5.2	Pro105−Ser207	11 442
11 840 ± 7.5	Ser2−Pro105	11 853
15 324 ± 10.3	Ser2−Ser135	15 289
15 355 ± 5.4	Ser2−Ala136	15 360
15 378 ± 12.3		
15 997 ± 10.9	Ser2−Leu142	16 015
16 060 ± 9.8	Ser2−Gly143	16 071
16 192 ± 13.6	Ser2−Cys144	16 175
16 536 ± 8.3	Ser2−Glu147	16 515
16 667 ± 7.4	Ser2−Asp148	16 631

[a] Masses with small deviations were assigned to the same fragment. [b] Assignments to polypeptide sequences are based on mass determination and sequencing data. [c] The theoretical molecular masses were calculated from the TetR(B) sequence assuming hydrolysis of the respective peptide bonds. [d] This mass was assigned to a C-terminal fragment.

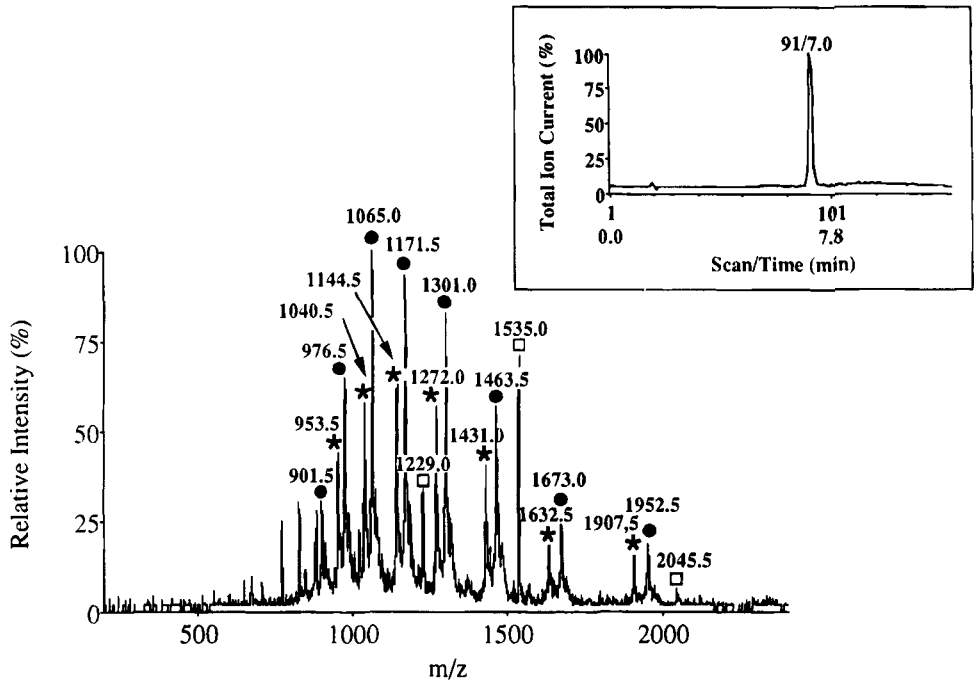

FIGURE 6: Positive electrospray mass spectrum of the main cleavage fragments. The composition of the most abundant cleavage products obtained by averaging four scans is shown. Mass peaks labeled with a filled circle, an asterisk, and an open square designate differently charged ions corresponding to a mass of 11 705 (6−13-fold), 11 436 (6−12-fold), and 6136 Da (3−5-fold), respectively. The total ion current chromatogram of the same sample obtained by HPLC−MS is depicted in the inset. Three main components coelute from the C_{18} column at approximately 7.0 min.

in the presence of Fe^{2+} within the first 30 s of the reaction. This yield was further reduced when the products were incubated with less Fe^{2+} (not shown). At longer reaction times a slow increase of yield was observed, resulting in about a doubling of the amount of product after 30 min. In contrast, the maximal cleavage yield was obtained within the first 30 s in the presence of tc−Fe^{2+}, and the yield was then slightly reduced when the reaction time was increased. We attribute this to nonspecific cleavage occurring at longer reaction times, which is consistent with an elevated background intensity observed on the respective gels (data not shown).

Denatured TetR Is Not Cleaved. The PAA gel in Figure 4 shows that treatment of denatured Tet repressor with a mixture of Fe^{2+} and tc and a 10-fold excess of H_2O_2/ascorbate for 15 s gave no cleavage, whereas treatment of native protein generated mainly fragments with molecular masses approximating 10 and 9 kDa (Ettner et al., 1993). Between 10% and 15% of TetR was cleaved under these conditions. Fragments of about 17, 15, 8, 7, and 5 kDa, respectively, were also observed but in lower yields.

Effect of Radical Scavengers on TetR Cleavage. The addition to the reaction mixture of several radical scavengers like glycerol, *tert*-butyl alcohol, and mannitol at concentrations of 0.5 M had no effect on the yield of cleavage as shown in Figure 4. The reaction in the presence of 0.5 M thiourea (lane 8) resulted in a decreased yield of cleavage products in comparison to the other scavengers, which may be explained by partial denaturation of Tet repressor at this concentration of thiourea. Thus, radical scavengers do not interfere with tc−Fe^{2+}-directed H_2O_2-dependent cleavage of TetR.

HPLC Analysis of the Cleavage Products. The mixtures containing cleaved fragments from control (no tc) and tc−Fe^{2+} reactions were separated on a reverse-phase HPLC C_4 column. The elution profiles are shown in Figure 5A,B. Samples containing tc−Fe^{2+} showed about 10-fold more cleavage product eluting at 21.5 min than the control without drug. The isolated fragments of the experiment shown in Figure 5A were analyzed by SDS−PAGE (Figure 5C).

No separation of the cleavage products from the intact Tet repressor was obtained when the reaction products of tc−Fe^{2+} cleavage were treated with 0.1% trifluoroacetic acid and subjected to reverse-phase HPLC. Cleaved peptides were separated from the intact protein only after denaturation of the reaction products by either heating or addition of urea and DTT. A gel filtration chromatography of the nondenatured cleavage products on Superose 12 showed no separation of cleaved fragments, either. These results indicate that TetR remains associated after the cleavage reaction and dissociates only after denaturation.

Sequence Analysis of the Cleavage Products. To determine the exact cleavage sites of the tc−Fe^{2+}-dependent reaction, we have analyzed the N-terminal sequence of the electroblotted peptides by Edman degradation. The N-terminal sequence of the 10-kDa peptide was Ser-Arg-Leu-Asp-Lys, identical with the N-terminus of native Tet repressor (Postle et al., 1984). The 9-kDa band gave rise to two N-terminal sequences, Pro-Thr-Glu-Lys-Gln and Thr-Glu-Lys-Gln-Tyr, in a molar ratio of about 1.2:1.0. These correspond to internal TetR peptides starting at residues 104 and 105, respectively. Edman degradation of peptides corresponding to the minor bands above and below the main cleavage products (see Figure 4) revealed only N-terminal fragments of the repressor. Furthermore, HPLC-purified fractions used for ESMS analysis (see below) were analyzed by N-terminal sequencing. Only in the sample containing the main cleavage products (Figure 5C, lane a) was the Pro-Thr-Glu sequence found in addition to the N-terminus of TetR, whereas only N-terminal sequences were found in the

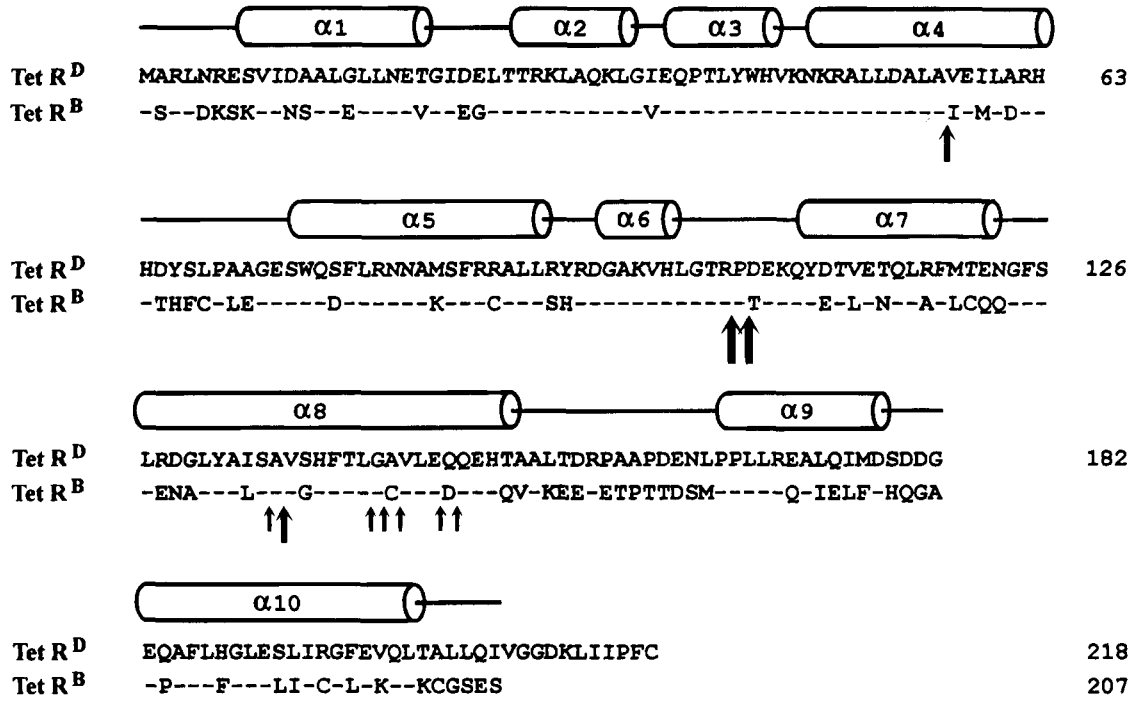

FIGURE 7: Location of cleavage sites in TetR(B) and sequence comparison with TetR(D). The amino acid sequences in the one-letter abbreviation of Tet repressors from two resistance determinants (upper, class D; lower, class B) are compared. The α-helical regions derived from the X-ray structure for TetR(D) are shown as open cylinders (Hinrichs et al., 1994). Dashes indicate identical residues in TetR(B) and TetR(D). Cleavage sites obtained with TetR(B) are indicated by arrows of different lengths representing different cleavage intensities.

other fractions (Figure 5C, lanes b−d). Sequence analyses of products from cleavage with Fe^{2+} in the absence of tc showed that the upper band in lane 2 of Figure 4 corresponds to the N-terminal portion of the protein. The amount of peptide in the lower band was too small to obtain a sequence.

Molecular Mass Determination of the Cleavage Products by ESMS. Cleavage reaction products separated by HPLC (see above) from the uncleaved protein were either applied directly to ESMS or rechromatographed using HPLC combined with ESMS for on-line mass analysis of eluted peptides (HPLC−MS). The first procedure led to a more accurate determination of masses because of scanning at a smaller step size and a longer dwell time. A typical example of the masses observed for the main cleavage products is displayed in Figure 6. A summary of the predominant masses along with their standard deviations is presented in Table 1. The accuracy of mass determinations for native TetR(B) was ±0.05%.

DISCUSSION

Activity of the tc−Fe^{2+} Complex. The Tn10-encoded tc resistance mechanism involves two proteins with specificity for the drug: TetA mediating active efflux of the drug and TetR regulating expression of TetA. The substrate for both proteins is tc chelated with any one of a variety of divalent ions. *In vitro* assays have demonstrated that tc−Co^{2+} is more efficiently transported into inverted versicles containing the efflux protein than tc−Mg^{2+} or tc−Ca^{2+} (Yamaguchi et al., 1990). Binding of tc to TetR requires the presence of divalent cations (Takahashi et al., 1986). The results presented here demonstrate that tc−Fe^{2+} is at least 1000-fold more active in induction than tc−Mg^{2+} (see Figure 1). Due to the TetR concentration of 2×10^{-7} M employed in this experiment this is the maximal enhancement of activity detectable under these conditions. Thus, the tc−Fe^{2+} activity may even be more than 1000-fold increased over tc−Mg^{2+}. The binding of Fe^{2+} to tc is about 100-fold stronger than that of Mg^{2+} (Martin, 1985). This indicates that TetR has

Table 2: Proximity Analysis of the Cleavage Sphere in TetR[a]

residue[b]	Mg···C=O[c] (Å) (deg)	Mg−C[d] (Å)	Mg−O[e] (Å)	W1[f] (Å)	W2[f] (Å)	W3[f] (Å)
Leu55	89.8	11.2	11.3	11.8	12.1	10.1
Ala56	81.5	8.6	8.5	9.6	9.7	7.5
Val57	87.5	10.6	10.6	11.9	11.7	9.4
His100	45.7	5.8	5.0	5.2	6.0	5.6
Leu101	125.5	6.7	7.5	5.2	6.9	6.7
Gly102	121.4	6.5	6.8	4.2	6.8	5.6
Thr103	61.1	4.6	4.2	3.5	5.9	3.6
Arg104	103.5	5.6	6.1	5.8	7.2	4.4
Pro105	119.2	7.8	8.5	8.5	9.4	6.5
Asp106	77.3	10.6	10.4	11.4	12.2	9.2
Ser135	57.8	9.0	8.4	9.4	7.7	10.6
Ala136	90.2	10.9	10.9	11.4	9.4	12.5
Val137	99.4	9.5	9.7	10.4	8.0	11.0
Ser138	90.2	7.3	7.4	7.9	5.8	8.9
Ser'135		20.0		20.0	18.5	21.5
Ala'136		18.5		18.4	17.0	20.1
Val'137		18.9		18.4	17.3	20.4
Leu'142	71.0	13.1	12.8	12.0	11.8	14.3
Gly'143	37.1	10.4	9.4	9.3	9.1	11.7
Ala'144	60.8	11.4	10.8	10.0	10.3	12.6
Val'145	78.8	12.4	12.2	10.7	11.5	13.3
Leu'146	96.1	10.2	10.4	8.4	9.5	10.9
Glu'147	77.4	8.8	8.6	6.8	8.3	9.5
Gln'148	100.8	11.6	11.9	12.2	13.3	12.1

[a] All distances and angles were derived from the crystal structure of TetR(D). [b] Amino acids marked with a prime indicate that the respective residue belongs to monomer 2. [c] Angles formed between Mg^{2+} and the carbonyl grouping. [d] Distances between Mg^{2+} and the carbonyl carbon. [e] Distances between the carbonyl oxygen of the peptide bond. [f] Distances between the oxygen atoms of each of the three waters and the carbonyl carbon of the respective residue.

FIGURE 8: Location of cleavage sites in the crystal structure of TetR(D)−tc−Mg^{2+}. (A, top) Stereoview of the structure of the entire TetR(D) dimer (Hinrichs et al., 1994) with the location of cleavage sites. The two monomers (yellow and pink) are depicted as solid ribbons. tc (cyan) is illustrated as a stick model with labeled oxygens 11 and 12 (red). The position of the Mg^{2+} is marked by a solid surface (blue). N-Terminal residues where cleavage sites are obtained are indicated by filled circles (red) of different size representing different cleavage intensities. The NH_2 and COOH termini are labeled N and C, respectively. (B, middle) Residues near cleavage sites within a radius of 20 Å around the metal ion (blue sphere) are shown for the dimer. The imidazole rings of His 100a and 100b (Nϵ sphere a in

an at least 10-fold preference for tc−Fe^{2+} compared with tc−Mg^{2+}. The marked increase of induction efficiency with Fe^{2+} raises the question of which counterion contributes to the inducing activity *in vivo*. While this cannot be decided on the basis of the available results, it is very clear that the TetR−tc−Fe^{2+} complex is functional in induction and is not artifactual. Thus, the results presented in this paper demonstrate for the first time that Fenton chemistry with Fe^{2+} in a functional complex with a protein can be a powerful tool to map residues of the protein which are in proximity to Fe^{2+}.

Cleavage Results from the Fenton Chemistry. The maximal yield of fragmentation of the protein occurs only in the presence of excess ascorbate and H_2O_2, showing that the multiple generation of the hyperreactive intermediate produced at the site of Fe^{2+} in the complex drives the cleavage reaction. Furthermore, the fast rate of the reaction is indicative of a highly reactive intermediate generated at the Fe^{2+} binding site and suggests also that the cleavage reaction is very specific for the proximity of Fe^{2+}. In comparison, treatment of the TetR−tc−Fe^{2+} complex with ascorbate/monoperoxyphthalic acid did not result in cleavage of the protein. This might be due to the negative charge and/or the increased size compared with H_2O_2. Thus, liganding of Fe^{2+} in the tc binding pocket of TetR may be limited to small molecules like water and H_2O_2.

Cleavage Occurs Specifically at Fe^{2+} in the TetR−tc−Fe^{2+} Complex. The fast cleavage reaction occurs only in the presence of native TetR protein (see also Figure 4), whereas denaturation of the protein prior to the reaction interferes with cleavage. Furthermore, the yield of cleavage products is severely reduced in the presence of excess Mg^{2+} (data not shown). A time course has shown that maximal cleavage occurs 1 h after the preformed TetR−tc−Mg^{2+} complex was challenged with an equimolar amount of Fe^{2+} (Ettner et al., 1993). The half-life of the TetR−tc−Mg^{2+} complex is about 15 min (Hillen et al., 1983). Thus, the time course indicates that the TetR−tc−Mg^{2+} complex has to dissociate before Fe^{2+} can replace Mg^{2+}. This observation also confirms the regionspecificity of the cleavage reaction.

The lack of an effect of several radical scavengers on the cleavage yield (see Figure 4) may indicate that hydroxyl radical formation is not involved in the cleavage reaction. As discussed in detail below, this is rather unlikely. Another explanation could be that the cleaved chemical bonds are in very close proximity of Fe^{2+}, so that their local concentration exceeds the ones obtained with the scavengers in the average diffusion path of the active oxo intermediates. In this case the results would support the interpretation that cleavage occurs in the proximity of a specifically bound Fe^{2+} in the TetR−tc−Fe^{2+} complex.

Determination of Cleavage Sites in the TetR−tc−Fe^{2+} Complex. The SDS−PAGE analysis (see Figure 4) shows clearly that a number of specific cleavage products are obtained with different yields. We performed two sets of experiments aimed at fine mapping of the cleaved sites. The first is N-terminal sequencing after blotting of the peptides to a membrane. The second approach makes use of ESMS. Since the cleavage reaction results in a variety of fragments spanning from 5 to 16 kDa, we were forced to perform intensive HPLC purification of the reaction products prior to ESMS. The interpretation of N-terminal sequencing and ESMS results is depicted in Figure 7. Most of the fragments started with the N-terminal sequence of TetR. Only two N-terminal sequences corresponding to the main cleavage products at amino acids 104 and 105, respectively, were identified. The masses of the corresponding two N-terminal fragments and one potential C-terminal fragment are present in the ESMS analysis (compare Table 1). This could indicate that the corresponding newly formed C-terminal TetR fragments contain modified residues at their respective N-termini, which may not be amenable to Edman degradation.

Assuming that the respective masses determined by ESMS correspond to N-terminal fragments of TetR, two more cleavage sites are identified. A minor cleavage site is at amino acid 56 in α-helix 4, and a number of cleavages occur in the region of residues 135, 136, 142, 143, 144, 147, and 148 in α-helix 8 (see Figure 7). This assignment accounts for all different masses revealed by ESMS (see Table 1). Masses corresponding to C-terminal fragments originating from the cleavage at these amino acids have not been found. This may be due to the HPLC purification where the larger fragments may coelute with the huge excess of uncleaved TetR, while the smaller fragments below 5.5 kDa are overcrowded by a large number of cleavage products, making it difficult to interpret the mass spectra of these samples. The most reliably determined masses support the assignment of cleavage sites shown in Figure 7.

Interpretation of the Cleavage Sites with Respect to the Crystal Structure of the TetR(D)−tc−Mg^{2+} Complex. The crystal structure of the TetR(D)−tc−Mg^{2+} complex has recently been solved (Hinrichs et al., 1994), providing the opportunity to structurally interpret the cleavage data. The sequences of both repressor proteins are shown in Figure 7. TetR(D) and TetR(B) share 65% sequence identity, and their three-dimensional structures have the same peptide folding (Hinrichs et al., 1994). The location of the cleavage sites are marked in the TetR(D) structure (Figure 8A). They are located in the core of the protein at the tc binding pocket in close proximity to the metal ion. No cleavage site was detected in the DNA binding domain, and the C-terminus of the protein was not affected by the cleavage mechanism. Table 2 contains the distances of the Mg^{2+} ion to the closest scissile peptide bonds defining the cleavage sphere (see also Figure 8B) as well as the angles formed by the C=O bonds with the line connecting the respective carbon atom and Mg^{2+}. In addition, the distances between each of the three water molecules liganding the metal ion and the respective carbonyl carbons in the peptide bonds have been determined

yellow and b in pink), the 11 and 12 oxygens (red sphere) of tc (cyan), and three water molecules (red spheres) are liganding the metal. Residues from subunit 1 in the TetR dimer are shown in yellow and residues from subunit 2 in pink. Helical portions are indicated by blue ribbons. (C, bottom left) Structure of the main cleavage sites at residues 104 and 105 with respect to the metal (Mg^{2+}) and water (W1, W2, W3) locations. The dotted white lines and respective numbers indicate the distances of the carbon in the respective peptide bonds to water W3. (D, bottom right) Capture of the second cleavage site around residue 147. The pink color indicates the other subunit in the TetR dimer compared to (C). Distances from water W3 to cleaved peptide bonds are indicated by white dotted lines with the respective distances indicated in angstroms.

and are also given in Table 2. The protein groupings surrounding the metal ions and the coordinating water molecules are shown for the TetR(D) dimer in Figure 8B. These data indicate that the residues located in closest proximity to the water molecules are predominantly cleaved. Specifically, water 3 is closest to the peptide bonds of residues 104, 105, and 56 in monomer 1 (Figure 8C) with 6.48, 4.35, and 7.50 Å, respectively. Activation of this water may lead to cleavage at these sites, yielding sequenceable new N-termini. The protein backbone at residues 100 and 103 is also close to water 3 (Figure 8C), but we do not see cleavage at these positions. This may be due to the fact that the oxygens of the respective C=O bonds point towards water 3 and the metal ion (Figure 8C), as indicated by the angles given in Table 2. Furthermore, the imidazole ring of His100 is located between water 3 and the peptide bond of residue 100 and may shield it from cleavage. Water 2 seems to be too far away from any of the peptide bonds of residues 100−106 and residues in α-helix 4 to contribute much to cleavage at these sites, whereas it is the closest water molecule to residues 135−138 in α-helix 8 (Table 2). In contrast, water 1 is the closest water molecule to residues 146 and 147 in α-helix 8 of monomer 2 and may cleave these sites (Figure 8D). The longer distances between waters 1 and 2 and these carbonyl carbons may account for the reduced site specificity of cleavage and the lower yield of the originating fragments as compared to the cleavages assigned to water 3. Furthermore, waters 1 and 2 are hydrogen bonded to the carboxylate side chain of Glu-147 and may therefore exchange more slowly with H_2O_2 compared to water 3.

The nucleophilic H_2O_2 binds to chelated Fe^{2+}, presumably by replacing one of the water ligands (Philip & Brooks, 1974). The binding mode of peroxide to iron depends on pH (Ahmad et al., 1988; Fujii et al., 1990). At pH 7.0 it binds most likely end-on, which would lead to an even reduced distance between oxygen of H_2O_2 and the cleaved peptide bond in TetR (see Table 2). Taken together, the tc−Fe^{2+}-dependent cleavage occurs at sites which are in close proximity to Mg^{2+} in the crystal structure. This finding clearly demonstrates the validity of this proximity analysis in general and supports the assumption that the crystal and solution structures are very similar, at least as far as the tc−Mg^{2+} binding pocket is concerned.

Mechanism of Fe^{2+}-Dependent Cleavage by H_2O_2. While it had been generally assumed that EDTA−Fe^{2+}-dependent cleavage of, e.g., DNA occurred by the action of hydroxyl radicals generated by Fe^{2+} to Fe^{3+} oxidation (Dixon et al., 1991), recent evidence by Rana and Meares (1991a) suggests a nonradical $Fe^{2+,3+}$-dependent mechanism of H_2O_2 activation for protein cleavage. This was based on the observation that cleavage induced by Fe^{2+} bound to a tethered EDTA was not inhibited by radical scavengers. In addition, it resulted in C-termini which contained oxygen from H_2O_2 and N-termini which were sequenceable by Edman degradation (Rana & Meares, 1991a; Ermácora et al., 1992). In agreement with these results we do not see an effect of radical scavengers on TetR cleavage. The ferrous ion in the TetR−tc−Fe^{2+} complex is part of a tightly bound substrate resulting in a specific binding mode compared to the EDTA−Fe^{2+} complex, which is only kept in close proximity to the substrate binding pocket by a tether. The distances of water molecules to the cleaved bonds derived from the crystal structure are so short (see Table 2) that a radical quencher might have only a negligible chance to scavange the radical and suppress cleavage. Thus, the lack of scavanging does not necessarily argue against involvement of radicals in the cleavage mechanism. The second observation that casts some doubt on a radical mechanism in the analysis presented here is the fact that we find cleavage products which are susceptable to Edman degradation. However, this is true for only one of the three regions of preferred cleavage.

Small amounts of cleavage products corresponding to molecular masses higher than 23 kDa, the molecular mass of the TetR monomer, are detected by PAGE (Figure 4). These bands can only be generated via cross-linking of cleaved peptides to uncleaved TetR in a reaction initiated by hydroxyl radicals as discussed by Kim et al. (1985). In addition, the fact that the masses of the fragments determined by ESMS deviate slightly from their theoretically expected values for peptide bond hydrolysis suggests that other reactions may take part in the cleavage. A similar result has recently been found for self-cleavage of a model peptide (Bateman et al., 1985; Platis et al., 1993). It is also conceivable that the hydrolysis of the peptide bond may be a secondary reaction after the initial attack by either a nucleophilic peroxide species or a hydroxyl radical.

Recent investigations of the reactive entity of Fe^{2+}/H_2O_2-mediated damage to macromolecules and saturated hydrocarbons point to an iron oxenoid (Fe^{V}=O) species as opposed to hydroxyl radicals (Jezewska et al., 1989). Furthermore, hydroxyl radicals are generated by Fe^{2+} preferably at low pH, while the evidence for their generation at the higher pH used here is less convincing (Rush & Koppenol, 1988). Taken together, we have no clear evidence to favor either the radical or activated oxo intermediate mechanism over the other. It seems rather likely that both mechanisms take place, resulting in only some new N-termini which are amenable to Edman degradation. We demonstrate clearly, though, that cleavage of TetR occurs at residues close to the location of Fe^{2+} in the induced complex. Thus, whatever the intermediate may be, it must be reactive enough to preferably undergo localized reactions with groupings in close proximity. Thus, the most important conclusion derived from our results is that cleavage of TetR directed by the active substrate tc−Fe^{2+} identifies residues located in the immediate proximity of the Fe^{2+} ion. This observation offers the possibility that proximity mapping of Fe^{2+} coordination may be possible in many more proteins containing Fe^{2+} binding sites.

ACKNOWLEDGMENT

We are grateful to Drs. Michael Niederweis, Weidong Ding, Sjaak Reumkens, Miguel Carrion, and Marshall M. Siegel for useful comments and discussions and to Doug B. Kitchen for his help with the computer modeling.

REFERENCES

Ahmad, S., McCallum, J. D., Shiemke, A. K., Appelman, E. H., Loehr, T. M., & Sanders-Loehr, J. (1988) *Inorg. Chem.* 27, 2230−2233.

Bateman, R. C., Jr., Youngblood, W. W., Busby, W. H., Jr., & Kizer, J. S. (1985) *J. Biol. Chem. 260*, 9088−9091.

Beck, K. P., Mutzel, R., Barbe, J., & Müller, W. (1982) *J. Bacteriol. 150*, 633−642.

Bertrand, K. P., Postle, K., Wray, L. V., Jr., & Reznikoff, W. S. (1983) *Gene 23*, 149−156.
Bruins, A. P., Covey, T. R., & Henion, J. D. (1987) *Anal. Chem. 59*, 2642−2646.
Dixon, W. J., Hayes, J. J., Levin, J. R., Weidner, M. F., Dombroski, B. A., & Tullius, T. D. (1991) *Methods Enzymol. 208*, 380−413.
Ermácora, M. R., Delfino, J. M., Cuenoud, B., Schepartz, A., & Fox, R. O. (1992) *Proc. Natl. Acad. Sci. U.S.A. 89*, 6383−6387.
Ettner, N., Ellestad, G. A., & Hillen, W. (1993) *J. Am. Chem. Soc. 115*, 2546−2548.
Fujii, S., Ohya-Nishiguchi, H., & Hirota, N. (1990) *Inorg. Chim. Acta 175*, 27−30.
Hecht, B., Müller, G., & Hillen, W. (1993) *J. Bacteriol. 175*, 1206−1210.
Heuer, C., & Hillen, W. (1988) *J. Mol. Biol. 202*, 407−415.
Heukeshoven, J., & Dernick, R. (1988) *Electrophoresis 9*, 28−33.
Hillen, W., & Berens, C. (1994) *Annu. Rev. Microbiol. 48*, 345−369.
Hillen, W., Klock, G., Kaffenberger, I., Wray, L. V., Jr., & Reznikoff, W. (1982) *J. Biol. Chem. 257*, 6605−6613.
Hillen, W., Gatz, C., Altschmied, L., Schollmeier, K., & Meier, I. (1983) *J. Mol. Biol. 169*, 707−721.
Hillen, W., Schollmeier, K., & Gatz, C. (1984) *J. Mol. Biol. 172*, 185−201.
Hinrichs, W., Kisker, C., Düvel, M., Müller, A., Tovar, K., Hillen, W., & Saenger, W. (1994) *Science 264*, 418−420.
Hoyer, D., Cho, H., & Schultz, P. G. (1990) *J. Am. Chem. Soc. 112*, 3249−3250.
Jezewska, M. J., Bujalowski, W., & Lohman, T. M. (1989) *Biochemistry 28*, 6161−6164.
Kim, K., Rhee, S. G., & Stadtman, E. R. (1985) *J. Biol. Chem. 260*, 15394−15397.
Koppenol, W. H. (1988) *J. Am. Chem. Soc. 110*, 4957−4963.
Martin, R. B. (1985) in *Metal Ions in Biological Systems*, Vol. 19, pp 19−52, Marcel Dekker, Inc., New York and Basel.
Maxam, A. M., & Gilbert, W. (1980) *Methods Enzymol. 65*, 499−559.
Niederweis, M., Lederer, T., & Hillen, W. (1992) *J. Mol. Biol. 228*, 322−326.
Philip, C. V., & Brooks, D. W. (1974) *Inorg. Chem. 13*, 384−386.
Platis, I. E., Ermácora, M. R., & Fox, R. O. (1993) *Biochemistry 32*, 12761−12767.
Postle, K., Nguyen, T. T., & Bertrand, K. P. (1984) *Nucleic Acids Res. 12*, 4849−4863.
Rana, T. M., & Meares, C. F. (1990) *J. Am. Chem. Soc. 112*, 2457−2458.
Rana, T. M., & Meares, C. F. (1991a) *Proc. Natl. Acad. Sci. U.S.A. 88*, 10578−10582.
Rana, T. M., & Meares, C. F. (1991b) *J. Am. Chem. Soc. 113*, 1859−1861.
Rush, J. D., & Koppenol, W. H. (1988) *J. Am. Chem. Soc. 110*, 4957−4963.
Schägger, H., & von Jagow, G. (1987) *Anal. Biochem. 166*, 368−379.
Schepartz, A., & Cuenoud, B. J. (1990) *J. Am. Chem. Soc. 112*, 3247−3249.
Smith, L. D., & Bertrand, K. P. (1988) *J. Mol. Biol. 203*, 949−959.
Takahashi, M., Altschmied, L., & Hillen, W. (1986) *J. Mol. Biol. 187*, 341−348.
Takahashi, M., Degenkolb, J., & Hillen, W. (1991) *Anal. Biochem. 199*, 197−202.
Tovar, K., & Hillen, W. (1991) *Methods Enzymol. 208*, 54−63.
Tullius, T. D., & Dombroski, B. A. (1986) *Proc. Natl. Acad. Sci. U.S.A. 83*, 5469−5473.
Unger, B., Klock, G., & Hillen, W. (1984) *Nucleic Acids Res. 12*, 7693−7703.
Yamaguchi, A., Udagawa, T., & Sawai, T. (1990) *J. Biol. Chem. 265*, 4809−4813.

BI940976M